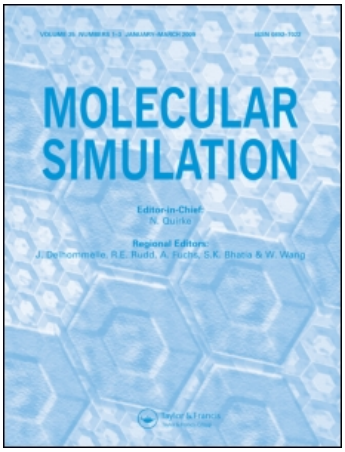

Molecular Simulation
Publication details, including instructions for authors and subscription information:
http://www.informaworld.com/smpp/title~content=t713644482

Conductance in Coulomb blockaded molecules—fingerprints of wave-particle duality?

B. Muralidharan[a]; A. W. Ghosh[b]; S. Datta[a]
[a] School of Electrical and Computer Engineering, Purdue University, West Lafayette, IN, USA [b] School of Electrical and Computer Engineering, University of Virginia, Charlottesville, VA, USA

To cite this Article Muralidharan, B. , Ghosh, A. W. and Datta, S.(2006) 'Conductance in Coulomb blockaded molecules—fingerprints of wave-particle duality?', Molecular Simulation, 32: 9, 751 — 758
To link to this Article: DOI: 10.1080/08927020600943923
URL: http://dx.doi.org/10.1080/08927020600943923

Molecular Simulation, Vol. 32, No. 9, 15 August 2006, 751–758

Taylor & Francis
Taylor & Francis Group

Conductance in Coulomb blockaded molecules—fingerprints of wave-particle duality?

B. MURALIDHARAN†*, A. W. GHOSH‡ and S. DATTA†

†School of Electrical and Computer Engineering, Purdue University, West Lafayette, IN 47907, USA
‡School of Electrical and Computer Engineering, University of Virginia, Charlottesville, VA 22904, USA

(Received June 2006; in final form June 2006)

In molecular electronics it is common to use the so called "NEGF-DFT" prescription where the mean-field describing electron–electron interactions is identified with the "Kohn–Sham potential" from density functional theory (DFT). However, a large number of experimentally observed molecular current–voltage (I–V) characteristics belong to the Coulomb blocade (CB) limit, and exhibit evidence of a rich interplay between charge quantization and size quantization, i.e. between particle and wave aspects of an electron. Although, NEGF-DFT techniques take into account the wave nature of electrons, they are essentially one-electron potentials and are inadequate to describe Coulomb blockade regime, especially under non-equilibrium conditions. Here, we present simple examples to illustrate the fact that such mean-field theories that may describe equilibrium properties do not necessarily describe non-equilibrium properties (like current flow) as well. While weak coupling with contacts and the associated *charge quantization* produce a suppressed zero-bias conduction or Coulomb Blockade followed by a staircase, *size quantization* generates an extensive body of single-particle excitations that create a quasiohmic rise in current with gateable onset voltages and symmetry properties. We discuss the underlying physics of these conduction processes using minimal models, starting with Coulomb blockade in a single spin-degenerate quantum dot, and subsequently the emergence of excitations in a double dot with singlet–triplet levels. The results bear compelling parallels with experimental results, underscoring the inadequacy of orthodox Coulomb blockade theory for size quantization, as well as traditional mean-field quantum transport calculations that only capture a small subset of the corresponding excitations within the molecular many-body Fock space.

Keywords: Molecular conduction; Coulomb blockade; NEGF-DFT; Fock space; Strong-correlations; Quantum-dots

1. Introduction

Molecular electronics represents an ultimate goal for materials science and device engineering, given the low cost of fabrication and tunability of mechanochemical properties. While its relevance to real-world devices and circuits is not yet clear, molecules do function as excellent laboratories for studying fundamental quantum physics. For example, low-bias mesoscopic experiments yield quantization of linear response parameters such as resistance, and thermal conductance [1,2]. In addition, far-from-equilibrium measurements can serve as an important spectroscopic tool for mapping out the molecular many-electron configuration space [3] as well as the effects of strong correlation on transport. The treatment of correlated transport would, require a re-evaluation of past theoretical treatments which have traditionally been formulated in the mean-field limit, for describing electron–electron interactions [4].

In this paper, we will refer to non-equilibrium Green's functions (NEGF) technique, as a class of theories that are a combination of Landauer style scattering theory with perturbative treatments of electron–electron and electron–phonon interactions [5]. Following the work of Keldysh, Kadanoff and Baym [6], they are usually corrected for electron–electron interactions through DFT. This is what we refer to generically as "standard NEGF" models [1,4]. This treatment has two major contributions: (a) inclusion of contacts through self-energies following the work of Caroli *et al.* [7]. This we consider as a part of "standard NEGF", and is now widely used following Meir *et al.* [8]. (b) A way to include strong electron–electron interactions by calculating the corresponding self-energy in a way that goes beyond standard NEGF is spelt out in Danielewicz [9]

*Corresponding author. Email: bmuralid@purdue.edu

Molecular Simulation
ISSN 0892-7022 print/ISSN 1029-0435 online © 2006 Taylor & Francis
http://www.tandf.co.uk/journals
DOI: 10.1080/08927020600943923

and Meir *et al.* [10]. This has not been developed further to our knowledge except for a few scattered papers [11]. In molecular electronics it is common to use this so called "NEGF-DFT" prescription where the mean-field describing electron–electron interactions is identified with the "Kohn–Sham potential" from density functional theory (DFT), which has been very successful in describing equilibrium properties. The purpose of this paper is to present simple examples to illustrate the fact that mean-field theories that describe equilibrium properties well do not necessarily describe non-equilibrium properties (like current flow) as well. More complicated real-world version of these examples have already appeared in the literature [12]. Our objective here is to convey the essential message as simply as possible.

The NEGF-DFT formulation has also been particularly successful for quantitative modeling of the current–voltage (I–V) characteristics of molecular wires with weak correlation effects [13–15], such as insulating alkanethiols [16], metallic quantum point contacts or nanotubes, silicon films and long conjugated molecules [17]. The approach, in essence, is to treat the molecule as a quantum wire with size quantization effects included through their quantized molecular wavefunctions, but ignoring in the process the particulate aspect of electrons. Metallic dots work in the opposite regime where charge quantization is included in an effective capacitor–resistor network [18], but the spread of the electronic wavefunction is ignored. A short, weakly bonded molecule can belong to a unique intermediate regime where the level broadening is comparable to the single electron charging energy, which in turn exceeds its semiconducting counterpart owing to the small size and dielectric constant of the molecular dot. Both charge and size quantization effects become important under these circumstances [19]. In fact, transport measurements in this regime does unearth a rich spectrum of many-electron signatures [20–24] that maybe hard to map onto their significantly reduced, one-electron subspace [12,25]. There is hence a motivation to develop quantum chemical and transport models in the many-electron (Fock) space [12,26–28].

As an example, let us consider benzene, whose capacitive charging energy $U \sim q^2/4\pi\epsilon_0 R \sim 2\,\mathrm{eV}$ ($R \approx 10\,\text{Å}$ is the radius of the benzene highest occupied molecular wavefunction) is an order or magnitude larger than the corresponding level broadening by either contact. The contact broadenings are given by Fermi's golden rule, $\Gamma_{1,2} = 2\pi|\tau_{\mathrm{Au-S}}|^2\ \rho_0|\langle\psi|\phi_{1,2}\rangle|^2$, where ρ_0 is the surface density of states of gold, $|\psi\rangle$ is the wavefunction whose broadening contribution is being investigated, $|\phi_{1,2}\rangle$ represent the atomic basis set localized on the end sulphur atoms and $\tau_{\mathrm{Au-Si}}$ is the gold–sulphur coupling evaluated in the local atomic basis set. For the HOMO wavefunction of benzene chemisorbed to gold, we use $\tau_{\mathrm{Au-S}} \approx 2\,\mathrm{eV}$ for the sulphur–gold coupling, $\rho_0 \approx 0.07\,\mathrm{eV}$ for the surface density of states of gold, and $1/\sqrt{8}$ [14] for the fraction of the HOMO wavefunction residing on the end sulphur atom, giving a broadening $\sim 100\,\mathrm{meV}$. The interlevel separation $\Delta\epsilon$ for benzene is also a few volts in magnitude, corresponding to the carbon–carbon covalent bonding energy. The order of magnitude estimates, consistent with detailed DFT calculations, show that short molecules typically satisfy $k_BT < \Gamma_{1,2} < \Delta\epsilon \leq U$, even assuming perfect chemisorption.

The inequality $U > \Gamma$ amounts to enforcing charge quantization by dictating that the contact resistances exceed the resistance quantum $2q^2/h$ (identifying the broadening Γ with a lifetime that is set by the RC time-constant of the molecule). On the other hand, the large interlevel separation $\Delta\epsilon$ compared to thermal or contact broadening enforces size quantization [18]. This effect enters through the quantum capacitance of the dot that describes size quantization or discreteness of the molecular density of states, and contributes to the RC time constant significantly by operating in series with the electrostatic capacitance of the dot. We therefore need a second-quantized transport formulation that can do complete justice to wave-particle duality, and the above regime will be our focus.

In this paper, we will argue that the careful consideration of many-electron effects in transport (a) yield results that are compellingly similar to a lot of experiments [20–21], and (b) are hard to capture with modified one-electron theories, even considering just qualitative trends for the simplest minimal quantum dot systems, indicating that approximate treatments that work for equilibrium are not guaranteed to work for non-equilibrium. We will first identify the full many-electron Hubbard Hamiltonian for an array of quantum dots representing the atoms constituting the molecule. The basis set is assumed to be minimal enough that the Hamiltonian is exactly diagonalizable and all many-electron effects, perturbative and non-perturbative, are automatically included. We will then develop rate equations [19] in this many-electron configuration space driven under bias by the contacts, assuming weak coupling. The resulting I–Vs will be studied for systems with progressively increasing degrees of sophistication. For a single quantum dot, we will see how electronic self-interaction correction [29–31] leads to a pronounced suppression in zero-bias conductance. While this can be captured with unrestricted mean-field results, discrepancies start manifesting themselves in the higher bias Coulomb staircase where subsequent spin addition (removal) processes carry varying amounts of current. This result, observed experimentally [32], turns out to be very hard to obtain from mean-field results, even with significant variability of parameters and self-consistent potential. Finally, we will show that a coupled array of dots with long-ranged Coulomb and hopping terms create excitations that appear as quasiohmic regions that compete with the Coulomb staircase, are gateable and flip asymmetry around the charge degeneracy points [24]. While some analogous features should be observable with electron–phonon interactions as well, the energy scales of these transitions are much smaller, and principally manifest themselves at lower bias.

2. Coulomb staircase in a single level quantum dot

2.1 Equilibrium

A molecule is essentially an array of atoms with long ranged electrostatic and quantum couplings. The simplest system to describes various transport effects is (figure 1(a)) a single electronic level with on-site energy ϵ_0 and Coulomb charging energy U, coupled to contacts which serve as reservoirs with electrochemical potentials μ_L and μ_R, respectively. The molecular Hamiltonian we will work with at present is the Hubbard Hamiltonian

$$\hat{H} = \epsilon_0 \hat{n} + U\hat{n}_\uparrow \hat{n}_\downarrow \tag{1}$$

Exact diagonalizing this Hamiltonian leads to four many electron states (figure 1(b)), a zero electron state $|00\rangle$ with energy 0, two one electron states $|01\rangle$ and $|10\rangle$ with energies ϵ_0, and a two electron state $|11\rangle$ with energy $2\epsilon_0 + U$. The states correspond, respectively, to an empty level, an up spin level, a down spin level, and a level doubly occupied with an up and a down spin. Equilibrium occupancies of these states are given by $P_N = e^{-\beta(E_N - \mu N)}/\Omega$, where $\beta = 1/k_B T$ is the inverse thermal energy, $\mu = E_F$ is the equilibrium contact Fermi energy or electrochemical potential, and $\Omega = \sum_N e^{-\beta(E_N - \mu N)}$ is the grand partition function. The average electron occupancy is then given by $\langle N \rangle = \sum_N N P_N$. One can bypass the many-electron Fock space treatment by employing a suitable self-consistent potential acting in the one-electron subspace, modifying the energies as

$$\tilde{\epsilon} = \langle \partial \hat{H}/\partial N \rangle. \tag{2}$$

The interacting term can be written as

$$\begin{aligned} H_{\text{int}} &= U\hat{n}_\uparrow \hat{n}_\downarrow \\ &= U/2 \sum_\sigma \hat{n}_\sigma \hat{n}_\sigma \\ &= (U/2) \sum_\sigma \hat{n}_\sigma (N - \hat{n}_\sigma) \\ &= (U/2) N \sum_\sigma \hat{n}_\sigma - (U/2) \sum_\sigma \hat{n}_\sigma^2 \\ &= UN(N-1)/2, \end{aligned} \tag{3}$$

where we have used the fact that $N = \sum_\sigma \hat{n}_\sigma$, and $\hat{n}_\sigma^2 = \hat{n}_\sigma$, since $\hat{n}$ can only take values of zero or one. The self-consistent potential is then given by $U_{\text{SCF}} = \partial H_{\text{int}}/\partial N = U(N - 1/2)$. For a given electrochemical potential, one guesses the value of N, uses it to calculate the SCF potential, and then calculates in turn the occupancy N of the level $\tilde{\epsilon} = \epsilon + U_{\text{SCF}}$ using the Fermi–Dirac distribution $f(\tilde{\epsilon}) = 1/[1 + e^{\beta(\tilde{\epsilon} - \mu)}]$, proceeding along this line until self-consistent convergence.

It is easy to see that the equilibrium occupancy plot N–μ is qualitatively different between the SCF and many-body results. In the former, the electron occupancy is a fractional amount, adiabatically changing from zero to two. In the many-body result, however, one does not simply multiply the results for one electron by two, but the electron occupancy changes abruptly between zero to one, followed by a plateau of width U over which the electrons are blockaded by the Coulomb interaction, after which the election number reaches two abruptly. One could capture this Blockaded effect using an *unrestricted* self-consistent potential (USCF) by dictating that the up and down spins do not feel potentials due to themselves, i.e. eliminate

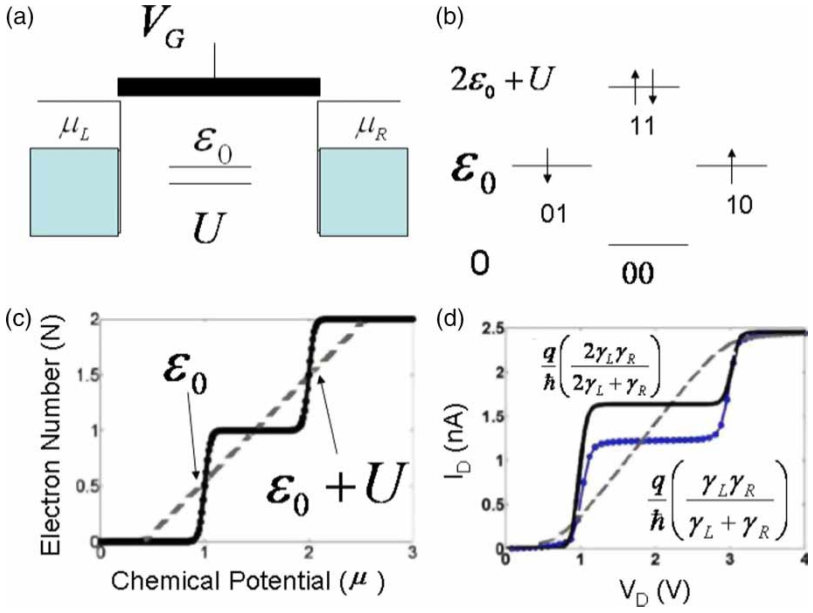

Figure 1. Comparison between SCF and CB regime of transport using (a) spin degree electronic level coupled to contacts. (b) The many-electron space comprises of 4 levels, (c) an Unrestricted SCF calculation introduces Self Interaction Correction which ultimately leads to integer transfer of electrons under equilibrium, however (c) fails to describe the fact that current plateaus have unequal heights (also see [12]) for addition or removal of consecutive electrons. Plateau widths however, can be adjusted by modifying the parameter U. Regular SCF calculations are also shown dashed in (b) and (c) for comparison.

electronic self-interaction. The potential for a particular spin is then given by $\langle \partial H_{\rm int}/\partial \hat{n}_\sigma \rangle = Un_\sigma = U(N - n_\sigma)$, with $n = \langle \hat{n} \rangle$ and $\bar{\sigma}$ represents the spin opposite to σ. This spin-dependent unrestricted potential eliminates the self-interaction of the level to which charge is being added. A self-consistent solution of the occupancy yields an N–μ plot very similar to the exact result, showing that an unrestricted calculation can capture *equilibrium* Coulomb Blockade effects.

2.2 Non-equilibrium

Non-equilibrium turns out to be hard to mimic with any SCF theory, even with considerable latitude in our choice of the SCF potential. Let us assume the contact injection rates are given by $\gamma_{1,2}/\hbar$, ignoring level broadening for the moment. One can write down a master equation for a transition from each many-electron level to each other, driven by the contacts, as follows

$$\dot{P}_i = -\sum_j R_{ij} P_i + \sum_j R_{ji} P_j \tag{4}$$

where i, j represent the many-body states $\{|00\rangle, |01\rangle, |10\rangle, |11\rangle\}$. The master equation, intuitively quite transparent from figure 2, can be formally derived by decoupling the contact and molecular density matrix equations in the steady state limit in the Markov approximation that ignores memory effects, and thus, energy dependent effects in the contact broadening. The transition rates are given by

$$\begin{aligned} R_{00\to 01} &= R_{00\to 10} = (\gamma_1 f_1 + \gamma_2 f_2)/\hbar \\ R_{01\to 00} &= R_{10\to 00} = (\gamma_1 f_1 + \gamma_2 f_2)/\hbar \\ R_{01\to 11} &= R_{10\to 11} = (\gamma_1 f'_1 + \gamma_2 f'_2)/\hbar \\ R_{11\to 01} &= R_{11\to 10} = (\gamma_1 f'_1 + \gamma_2 f'_2)/\hbar \end{aligned} \tag{5}$$

where $f_{1,2} = 1/[1 + e^{\beta(\epsilon_0 - \mu_{1,2})}]$, $f_{1,2} = 1 - f_{1,2}$, $f'_{1,2} = 1/[1 + e^{\beta(\epsilon_0 + U - \mu_{1,2})}]$, and $f'_{1,2} = 1 - f'_{1,2}$. In short, electron addition processes are governed by probability of occupancy f at the corresponding transition energies ϵ_0 or $\epsilon_0 + U$ by each contact electrochemical potential, while electron removal processes are governed by the probability of vacancy $1 - f$. At steady-state, it is straightforward to solve these equations (only three of which are independent), along with the normalization $\sum_i P_i = 1$. The probabilities are then used to calculate the current injected by one contact (say the left one) as

$$I^L = \sum_i (\pm e/\hbar) \left[-\sum_j R^L_{ji} P_i + \sum_j R^L_{ji} P_j \right] \tag{6}$$

where the rates R^L are obtained by only considering the individual left contact contribution to the corresponding rate, for example, $R^L_{00\to 10} = \gamma_1 f_1/\hbar$.

The SCF current is obtained by solving the rate equations in the one-electron subspace. The electron occupancy is given by $N = (\gamma_1 f_1 + \gamma_2 f_2)/(\gamma_1 + \gamma_2)$, where the Fermi functions are evaluated at the energy $\tilde{\epsilon} = \epsilon + U_{\rm SCF}$. The SCF potential in turn depends on N as before, so the calculation is done self-consistently. The converged Fermi functions are then used to calculate the current as $I = (2e/\hbar)\gamma_1\gamma_2/(\gamma_1 + \gamma_2)[f_1 - f_2]$. In the USCF limit, we keep track of individual spin potentials, and instead of multiplying the individual spin currents by two, add their contributions separately.

The RSCF model that treats spins equally tends to give an adiabatically increasing current that reaches its maximum contact-dominated value $2e/\hbar \times \gamma_1\gamma_2/(\gamma_1 + \gamma_2)$ when the contact electrochemical potential fully crosses the level. It is important to note that charging alone can smear the current, leading to a low conductance value spread out over a wide voltage range comparable to U. The RSCF potential $U(N - 1/2)$ causes a continuous shift in levels with charge addition, which is fractional. In contrast in the USCF regime and in the many body regime, current onset is abrupt. The USCF potential Un_σ does not show any shift in levels when the spin σ is added, until an additional voltage of U where the addition of the subsequent spin $\bar{\sigma}$ becomes feasible and the electron number jumps from one to two. Although this aspect of Coulomb Blockade seems to be in agreement with the exact result, the discrepancy arises when one looks at the current levels. The exact solution of the above equations yields a current plateau whose height is $\gamma_1\gamma_2/(2\gamma_1 + \gamma_2)$ in the large charging ($U \to \infty$ limit) which yields a value two-thirds of the maximum current, in contrast with the SCF result that gives a factor of half. If we kept track of

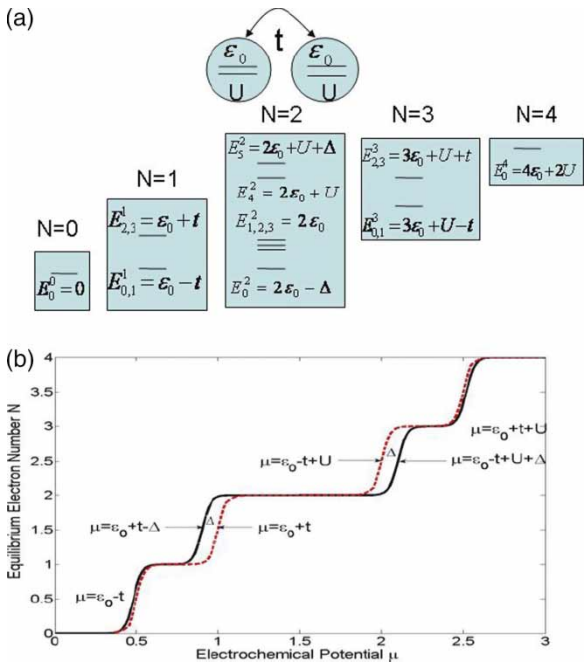

Figure 2. Many-electron spectrum and equilibrium properties of a coupled quantum dot system: (a) the $2^4 = 16$ energy levels are distributed amongst various charging configurations. (b) In comparison to an unrestricted scheme (dotted) the many body N–μ calculation (bold) has an earlier onset for the $N = 2$ plateau resulting from the singlet–triplet correlation energy Δ. One could in principle capture this correlation energy at equilibrium via SCF schemes by introducing appropriate correlation terms.

the entire many-electron configuration space, we would see that the discrepancy arises because there are two ways of adding the first spin and only one way of adding the second, a subtlety that is completely washed away when we choose to work in a reduced $N \times N$ (or $2N \times 2N$ for unrestricted) subspace instead of the full $2^{2N} \times 2^{2N}$ configuration space, thereby losing track of individual spin addition and removal channels.

The SCF potential ($\partial H/\partial n$) was calculated by writing the electron operators $\hat{n} = \langle \hat{n} \rangle + \delta\hat{n}$, expanding the Coulomb term $U\hat{n}_\uparrow\hat{n}_\downarrow$ and dropping the correlation terms $\delta\hat{n}_\uparrow\delta\hat{n}_\downarrow$ completely, i.e. the Hartree–Fock approximation. One could include parts of the correlation term phenomenologically, by dictating that $\hat{n}_i\hat{n}_j \approx (1 - g_{ij})\langle n_i \rangle\langle n_j \rangle$, with g_{ij} representing the exchange-correlation hole. This is in the spirit of Kohn–Sham theory, where the potential is calculated by various approximate means. However, the effect of g is simply to renormalize the charging energy U that it adjoins, influencing at best the *width*, but not the *height* of the current plateaus.

The situation gets more dramatic if we have asymmetric contacts $\gamma_1 \gg \gamma_2$. For equal coupling, each contact reached a balancing act between filling and emptying the level. For a positive bias on the weaker contact, the stronger contact keeps the level filled (which it can do in two ways, adding an up or a down spin, assuming the level was empty to begin with). For opposite bias, the stronger contact empties this level, which can now be done in only one way (up OR down depending on what occupied the level). The I–V is thus expected to be strongly as asymmetric, with the first plateau half the second for positive bias on the weaker contact, and merging with the second for opposite bias. This ratio of one to two, observed experimentally [32], arises in a straightforward way from our analyses since the ratio of the first and second plateau currents is given for positive bias by $(\gamma_1 + \gamma_2)/(2\gamma_1 + \gamma_2) \approx 1/2$ for $\gamma_1 \gg \gamma_2$, and by $(\gamma_1 + \gamma_2)/(\gamma_1 + 2\gamma_2) \approx 1$ for negative bias. The asymmetry arises from the difference in the number of spin addition and removal channels for positive and negative bias, and leads to an asymmetry in the current levels, in contrast to the SCF limit where current levels stay symmetric but the widths over which the currents saturate are different. Thus, *even for the simplest quantum dot, unrestricted potentials in the one-electron subspace cannot capture the non-equilibrium properties correctly.* We will next show that the situation gets worse for multiple dots or for dots with multiple orbitals, where additional physics due to correlations and excitations start to arise.

3. Double quantum dot: correlations at equilibrium

In short molecules the interplay between charging and hybridization generates a variety of effects in the many-electron spectrum, including a lowering of ground state energies due to correlation and the creation of electronic excitations within each charging configuration. Let us consider a simple example of a coupled quantum dot (figure 2(a)) with on-site energy $\epsilon_0 = 0.75\,\text{eV}$ and hopping parameter $t = 0.25\,\text{eV}$. For the moment, consider only an on-site Coulomb interaction $U = 1.5\,\text{eV}$ such that the Hamiltonian of this system is generally described as:

$$\hat{H} = \sum_i \epsilon_i \hat{n}_i - \sum_{ij} t_{ij}(c_i^\dagger c_j + hc) + \frac{1}{2}\sum_i U_i \hat{n}_{i\uparrow}\hat{n}_{i\downarrow} \qquad (7)$$

where $\hat{n}_i = \hat{n}_{i\uparrow} + \hat{n}_{i\downarrow} = \sum_\sigma \hat{n}_{i\sigma}$. It is straightforward to diagonalize the one-election Hamiltonian. However, in this case the many-electron Hamiltonian is exactly solvable, by diagonalizing subspaces of 0, 1, 2, 3 and 4 electrons. The 6×6 2-electron Hamiltonian is the non-trivial part, which leads to singlets, and triplets [33]. The energy levels E_i^N corresponding to each N-electron sector (charge configuration) are obtained as follows, assuming a common onsite energy ϵ_0 and Coulomb term U:

$$\begin{aligned}
&E_0^0 = 0\\
&E_{0,1,2,3}^1 = \epsilon_0 \pm t, \epsilon_0 \pm t\\
&E_{0,1,2,3,4,5}^2 = 2\epsilon_0 - \Delta, 2\epsilon_0, 2\epsilon_0, 2\epsilon_0, 2\epsilon_0 + U, 2\epsilon_0 + U + \Delta\\
&E_{0,1,2,3}^3 = 3\epsilon_0 + U \pm t, 3\epsilon_0 + U \pm t\\
&E_0^4 = 4\epsilon_0 + 2U
\end{aligned} \qquad (8)$$

where the singlet formation energy $\Delta = \sqrt{U^2/4 + 4t^2} - U/2 \approx 4t^2/U$ for large charging energy $U \gg t$.

The above spectrum allows for the calculation of transition points in the N–μ plot shown in figure 2(b). The one-electron transitions executed by the electrons under bias correspond to differences between the many-electron energies, $\epsilon_{ij}^{Nr} = E_i^N - E_j^{N-1}$ for removal levels, and $\epsilon_{ij}^{Na} = E_i^{N+1} - E_j^N$ for addition levels. It is easy to see that $\epsilon_{ij}^{Na} = \epsilon_{ij}^{N+1,r}$. At equilibrium only the ground state energies matter when $\mu = \epsilon_{00}^{Nr} = E_0^N - E_0^{N-1}$ allowing for a charge transfer between $N - 1 \rightarrow N$ electrons. These are given by $\epsilon_{00}^{Nr} = E_0^N - E_0^{N-1}$, and have values $\epsilon_{00}^{0r} = \epsilon_0 - t$, $\epsilon_{00}^{1r} = \epsilon_0 - \Delta + t$, $\epsilon_{00}^{2r} = \epsilon_0 + U - t + \Delta$ and $\epsilon_{00}^{3r} = \epsilon_0 + U + t$. As expected, the largest plateau in the N–μ plot (figure 2(b), black curve) is given by the two electron subspace, with width equal to $\epsilon_{00}^{2r} - \epsilon_{00}^{1r} = U + 2\Delta - 2t$. A Hartree Fock treatment of the Hamiltonian which includes self interaction correction (figure 2(b), red curve) results in a gap of $U + 2t$, missing the correlation energy of 2Δ. Technically various levels of SCF with adjustable g_{ij} could add correlation terms to the Hamiltonian eventually resulting in the correct transition energies. In the following part of the paper, we point out that while this may work for equilibrium, this alone would not suffice under non-equilibrium.

4. Double quantum dot: excitations under non-equilibrium conditions

Consider a double dot coupled to each other with coupling t, and to two different contacts with coupling strengths $\gamma_L = \gamma_R = 1\,\text{meV}$. A molecule is typically in a

configuration filled upto the HOMO level as shown in figure 3(a). When the two contacts are maintained at different chemical potentials, the calculation of currents utilizes the energy spectrum which floats according to a self consistent calculation of average electron concentration. In the Coulomb Blockade regime, weak coupling usually permits only integral charge transfer and thus a current plateau is activated only when a single electron level appears within the bias window. Owing to a larger many-electron spectrum, one expects even in this simple case several accessible transport channels. Let us consider two electrons in the equilibrium configuration of the double dot, corresponding to a half filled system. For the chosen parameter set, given a bias of the order of a couple of volts, electronic transitions occur only between neighboring charge spaces, i.e. between the neutral and singly ionized molecular configurations. We now depict transport that occurs via current plateaus whose current onsets are triggered when a removal level appears in the bias window. An I–V characteristic consisting of four plateaus is shown in figure 3(d), where the plateau onsets occur when either μ_L or μ_R crosses various transitions shown in the energy diagram of figure 3(c). It is crucial to note that only the first transition is caused due to a ground state transition or Coulomb removal. All subsequent steps are due to transitions involving various excited states. For example, the very second step is caused when the electron is re-injected into the system by the left contact into the excited triplet E_1^2 when $\mu_L > \epsilon_{10}^{2r}$, as shown in figure 2(a). Complete removal of a second electron from this system may take a few more volts resulting in a di-cation, usually not stable for a molecule. It is reasonable to expect that a huge body of such excitations (vibrational and electronic) will produce very closely spaced plateaus ultimately resulting in a quasilinear current rise. This has been observed in several experiments. It must be added that current onset close to zero bias in figure 3(d) is due to the fact that equilibrium Fermi energy is very close to the threshold transition ϵ_{00}^{2r}. We now turn to transport resulting due to varying initial condition E_F, usually possible by gating or having a different metallic contact.

Mapping the excitations: Coulomb Diamonds By plotting conductance voltage characteristics for different gate potentials one arrives at a Coulomb Blockade diamond [35]. Figure 4 shows a color plot of the molecular conductance as a function of the *local* drain and gate voltages V_D and V_G respectively. Note that these axial values are different from the applied voltages due to the involvement of a non-trivial voltage-division factor. This depends on the capacitance ratio, and thus on the channel to oxide aspect ratio and their dielectric constants. The slopes of the lines shows the transfer factor that describes how much drain voltage is needed to move a contact electrochemical potential into resonance with a level, when the level has already been shifted by the applied gate bias. It is easy to see how the various transition processes get mapped out in the Coulomb Blockade diagram. The lines (describe) arise from the ground-state to ground-state transition and are the most prominent lines, but in addition there are weaker parallel lines that arise due to excitations.

It is easy to see the nature of the $I - V_D$ or $I - V_G$ curves by taking a cut from the Coulomb Blockade diagram, which provides a compact, elegant way to incorporate the wealth of transition information that characterizes these molecular transitions. One finds two sets of curves—one where the current onsets are followed by clear plateaus, and the other where the current launches into a quasi-ohmic linear rise with voltage immediately upon onset. The flat plateaus are associated with ground-state to ground-state transitions, while the linear regimes arise from an abundance of closely spaced excitations that were already energetically accessible, but so far had non-existence matrix elements

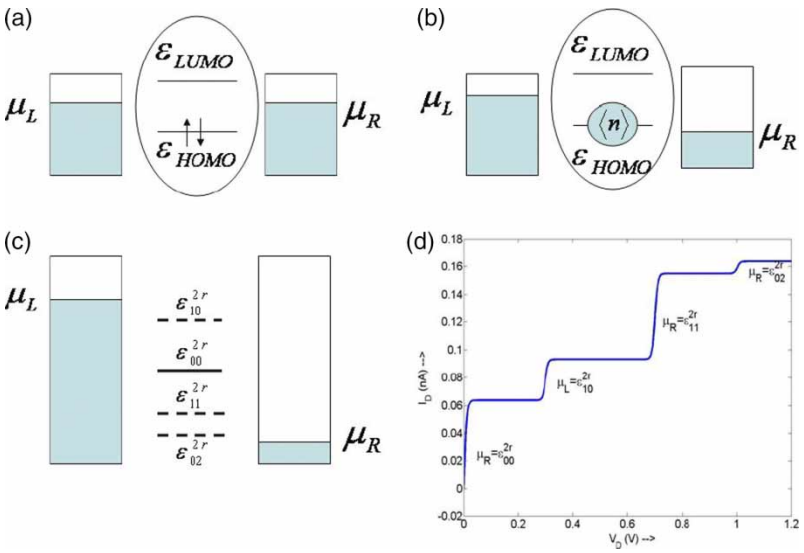

Figure 3. Transport in a coupled quantum dot: Onset of excitations (a) A neutral molecule is filled upto its HOMO orbital, in our case a doubly filled bonding orbital. (b) A self consistent calculation under non-equilibrium evaluates the non-equilibrium electron density to calculate currents. (c) Energy diagram for the typical CB I–V shown in (d) Note the majority of plateaus result from excitations. It takes beyond a few volts more to further ionize the system.

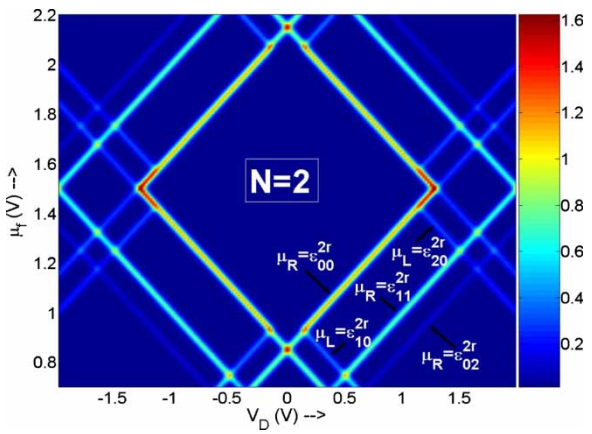

Figure 4. Coulomb Diamond for a coupled dot molecule. A conductance plot with varying gate voltage. Threshold and thus the zero current region varies as threshold channel, i.e. ε^{Nr}_{00} for the lower half or ε^{Na}_{00} for the upper half becomes energetically distant from E_F. The $N = 2$ indicates the number of electrons that is stabilized by the Coulomb Blockade region. Transitions involving removal spectrum (lower half) are mapped to display a general trend. The diamond usually can provide key information regarding the position of low lying excitations at least.

for transition because the ground-states had not yet been populated. It seems thus that depending on the position of the excitations, one could get only flat plateaus [34], or quasi-linear current rises [12].

5. What about effective one-electron potentials?

In this weakly coupled, strongly interacting regime of transport, non-trivial quantum interference effects arise under bias between interacting many-electron levels that are hard to describe through effective one-electron potentials. In a system described by an N orbital basis set, for example, all potentials are $N \times N$ in size with N eigenenergies ($2N$ if spin is considered). In contrast, the corresponding many-body Fock space involves transitions between 4^N states. While certain chemical properties such as molecular geometry and thermochemistry depend only on the ground-state properties, it may be hard to capture the entire wealth of information contained in this large Fock space, and its corresponding transport signatures, through just N eigenstates. At the least, one will need an energy-dependent self energy $\Sigma(E)$ whose poles will take care of the multiple transition levels and excitations not captured by the N eigenstates of the one-electron potential. Indeed, there have been attempts to include correlation by solving equations of motion for the electronic Green's function [8,10], using the full many-body Hamiltonian to extract the temporal evolution. Truncating the infinite hierarchy at various levels, corresponding to various levels of approximation, indicates the gradual emergence of physical effects associated with correlation. At the lowest order, one recovers the mean-field result through the one-electron Hamiltonian [29]. At the next level of hierarchy, one averages the Green's function instead of the Hamiltonian, indicating the need to deviate from a one-electron potential. At this level, one obtains the formation of local moments. At the next level, imposing a Hartree–Fock approximation only on the contact electrons and setting their correlations by their Fermi functions, we get a high-temperature Kondo result [10,11]. Indeed, a proper treatment of Kondo requires the self-energies to be Fermi-function dependent, while an applied bias further renormalizes the broadenings. At low temperatures, this hierarchy needs a different treatment by selectively summing a class of most divergent Green's functions (the non-crossing approximation) using the Renormalization Group Theory, yielding the correct low-temperature Kondo results [36]. It is thus quite clear that correlations cannot be captured simply by averaging Hamiltonians, but may need more sophisticated and possibly non-perturbative averaging procedures for the Green's function matrices [37–40].

6. Conclusion

The main point of the paper was to caution the reader that description of molecules in the Coulomb Blockade regime involves duality between charge and size quantization, and could have non-trivial transport effects often seen in experiments, that are hard to capture with an effective one-electron potential. We have described in detail using simple examples this regime of molecular conduction and what makes it conceptually difficult such that description within a standard NEGF (Landauer style) formalism fails. While our formalism handles these effects systematically, it misses the influence of (a) coherence between levels which would require using a many-electron density matrix [41], and (b) broadening of the level transitions [37–40] that are important for obtaining the charge quantization limit. A novel theory is needed to handle both these effects and could potentially provide insight into strong localization coupled with interactions.

References

[1] S. Datta. *Electronic Transport in Mesoscopic Systems*, Cambridge University Press, New York (1995) and references therein.
[2] L.G.C. Rego, G. Kirczenow. Quantized thermal conductance of dielectric quantum wires. *Phys. Rev. Lett.*, **81**, 232 (1998).
[3] J. Park, A.N. Pasupathy, J.I. Goldsmith, C. Chang, Y. Yaish, J.R. Petta, M. Rinkoski, J.P. Sethna, H.D. Abruna, P.L. McEuen, D.C. Ralph. Coulomb blockade and the Kondo effect in single-atom transistors. *Nature*, **417**, 722 (2002).
[4] S. Datta. *Quantum Transport: Atom to Transistor*, Cambridge University Press, New York (2005).
[5] G.D. Mahan. Quantum transport equation for electric and magnetic fields. *Phys. Rep.*, **145**, 251 (1987).
[6] H. Haug, A.-P. Jauho (Eds.). Quantum kinetics in transport and optics of semiconductors. *Springer Series in Solid-State Sciences*, 123, Springer-Verlag, Berlin, Heidelberg (1996).
[7] C. Caroli, R. Combescot, P. Nozieres, D. Saint-James. A direct calculation of the tunnelling current: IV. Electron–phonon interaction effects. *J. Phys. C: Solid State Phys.*, **5**, 21 (1972).
[8] Y. Meir, N.S. Wingreen. *Phys. Rev. Lett.*, **68**, 2512 (1992).
[9] P. Danielewicz. *Ann. Phys.*, **152**, 239 (1984).
[10] Y. Meir, N.S. Wingreen, P.A. Lee. *Phys. Rev. Lett.*, **66**, 3048 (1991).
[11] R. Swirkowicz, J. Barnas, M. Wilczynski. *Phys. Rev. B*, **68**, 195318 (2003) and references therein.

[12] B. Muralidharan, A.W. Ghosh, S. Datta. *Phys. Rev. B*, **73**, 155410 (2006).
[13] M. Di Ventra, S.T. Pantelides, N.D. Lang. *Phys. Rev. Lett.*, **84**, 979 (2000).
[14] P.S. Damle, A.W. Ghosh, S. Datta. *Chem. Phys.*, **281**, 171 (2002).
[15] J. Taylor, H. Guo, J. Wang. *Phys. Rev. B*, **63**, 215407 (2001).
[16] A.W. Ghosh, P.S. Damle, S. Datta, A. Nitzan. *MRS Bull.*, **29**, 391 (2004).
[17] F. Zahid, A.W. Ghosh, M. Paulsson, E. Polizzi, S. Datta. Charging-induced asymmetry in molecular conductors. *Phys. Rev. B*, **70**, 245317 (2004).
[18] H. Grabert, M.H. Devoret (Eds.). *Single Charge Tunneling*. NATO ASI Series 294, Plenum Press, New York (1992).
[19] E. Bonet, M.M. Deshmukh, D.C. Ralph. Solving rate equations for electron tunneling via discrete quantum states. *Phys. Rev. B*, **65**, 045317 (2002); C.W.J. Beenakker, *Phys. Rev. B*, **44**, 1646 (1991).
[20] J. Reichert, H.B. Weber, M. Mayor, H.v. Lohneysen. *Appl. Phys. Lett.*, **82**, 4137 (2003).
[21] M. Mayor, H.B. Weber, J. Reichert, M. Elbing, C. von Hisch, D. Beckmann, M. Fischer. *Angewandte Chemie Int. Ed.*, **42**, 5834 (2003).
[22] M. Elbing, R. Ochs, M. Koentopp, M. Fischer, C. von Hanisch, F. Evers, H.B. Weber, M. Mayor. *Proc. Natl. Acad. Sc.*, **102**, 8815 (2005).
[23] M.A. Reed, C. Zhou, D.J. Muller, T.P. Burgin, J.M. Tour. *Science*, **278**, 252 (1997).
[24] G.D. Scott, K.S. Chichak, A.J. Peters, S.J. Cantrill, J. Fraser Stoddart, H.-W. Jiang. cond-mat/0504345 (2005).
[25] R. Gaudoin, K. Burke. *Phys. Rev. Lett.*, **93**, 173001 (2004).
[26] M.H. Hettler, W. Wenzel, M.R. Wajewijs, H. Schoeller. Current collapse in tunneling transport through benzene. *Phys. Rev. Lett.*, **90**, 076805 (2003).
[27] B. Muralidharan, A.W. Ghosh, S.K. Pati, S. Datta. in preparation.
[28] P. Delaney, J.C. Greer. Correlated electron transport in molecular electronics. *Phys. Rev. Lett.*, **93**, 036805 (2004).
[29] J.J. Palacios. *Phys. Rev. B*, **72**, 125424 (2005).
[30] C. Toher, A. Fillipetti, S. Sanvito, K. Burke. *Phys. Rev. Lett.*, **95**, 116402 (2005).
[31] P. Pals, A. MacKinnon. *J. Phys.: Condens. Matter.*, **8**, 5401 (1996).
[32] M.M. Deshmukh, E. Bonet, A.N. Pasupathy, D.C. Ralph. Equilibrium and nonequilibrium electron tunneling via discrete quantum states. *Phys. Rev. B*, **65**, 073301 (2002).
[33] P. Fulde (Ed.). Electron correlations in molecules and solids. Springer Series in Solid-State Sciences, Vol. 100, Springer-Verlag, Berlin, Heidelberg (1991).
[34] J.-O. Lee, G. Lientschnig, F. Wiertz, M. Struijk, R.A.J. Janssen, R. Egberink, D.N. Reinhoudt, P. Hadley, C. Dekker. Absence of strong gate effects in electrical measurements on phenylene-based conjugated molecules. *Nano Lett.*, **3**, 113 (2003).
[35] W.G. van der Weil, S. DeFranceschi, J.M. Elzerman, T. Fujisawa, S. Tarucha, L.P. Kouwenhoven. *Rev. Mod. Phys.*, **75**, 1 (2003) and references therein.
[36] H.R. Krishnamurthy, K.G. Wilson, W. Wilkins. *Phys. Rev. Lett.*, **35**, 1101 (1975).
[37] S. Datta. cond-mat, 0603034. Fock space formulation for nanoscale electronic transport (2006).
[38] J. Koenig. *Quantum Fluctuations in a Single-Electron Transistor*, Dissertation, Shaker Verlag, Aachen (1999).
[39] S.A. Gurvitz, Y.S. Prager. Microscopic derivation of rate equations for quantum transport. *Phys. Rev. B*, **53**, 15932 (1996).
[40] J.N. Pedersen, A. Wacker. Tunneling through nanosystems: Combining broadening with many-particle states. *Phys. Rev. B*, **72**, 195330 (2005).
[41] S. Braig, P.W. Brouwer. Rate equations for Coulomb blockade with ferromagnetic leads. *Phys. Rev. B*, **71**, 195324 (2005).